Application of a non-linear k-ε model in prediction of convective heat transfer through ribbed passages

M. Raisee and A. Noursadeghi
Department of Mechanical Engineering, University of Tehran, Tehran, Iran
H. Iacovides
Department of Mechanical, Aerospace and Manufacturing Engineering, UMIST, Manchester, UK

Received September 2002
Revised June 2003
Accepted July 2003

Keywords *Flow measurement, Heat transfer, Turbulence, Modelling*

Abstract *A numerical investigation has been undertaken to study fluid flow and heat transfer through artificially rib-roughened channels. Such flows are of particular interest in internal cooling of advanced gas turbine blades. The main objective is to test the suitability of recently developed variants of the cubic non-linear k-ε model for the prediction of cooling flows through ribbed passages. The numerical approach used in this study is the finite-volume method together with the SIMPLE algorithm. For the modelling of turbulence, the Launder and Sharma low-Re k-ε model and a new version of the non-linear low-Re two equation model that have been recently shown to produce reliable thermal predictions in impinging jet flows and also flows through pipe expansions, have been employed. Both models have been used with the form of the length-scale correction term to the dissipation rate originally proposed by Yap and also more recently developed differential version, NYap. The numerical results over a range of flow parameters have been compared with the reported experimental data. The mean flow predictions show that both linear and non-linear k-ε models with NYap can successfully reproduce the distribution of the measured streamwise velocity component, including the length and width of the separation bubble, formed downstream of each rib. As far as heat transfer predictions are concerned, the recent variant of the non-linear k-ε leads to marked improvements in comparison to the original version of Craft et al. Further improvements in the thermal prediction result through the introduction of a differential form of the turbulent length scale correction term to the dissipation rate equation. The version of the non-linear k-ε that has been shown in earlier studies to improve thermal predictions in pipe expansions and impinging jets; it is thus found to also produce reasonable heat transfer predictions in ribbed passages.*

Nomenclature

A	= cross-section at area	h	= rib height
EVM	= Launder and Sharma low-Re linear k-ε	H	= channel height
		k	= turbulent kinetic energy
C_p	= specific heat transfer capacity of the fluid	$\dot{m}$	= mass flow rate
		NLEVM1	= original non-linear k-ε proposed by Craft *et al.* (1996)
D	= diameter of ribbed pipe		

International Journal of Numerical Methods for Heat & Fluid Flow
Vol. 14 No. 3, 2004
pp. 285-304

0961-5539
DOI 10.1108/09615530410517968

NLEVM2 = Recent version of non-linear k-ε proposed by Craft *et al.* (1999)
Nu = Nusselt number
NYap = differential form of Yap term recently modified by Craft *et al.* (1999)
p = pitch of the ribs
Pr = molecular Prandtl number
q_w = local surface heat flux on the wall
R = pipe radius
Re = Reynolds number
U_i = mean velocity components (U, V)
U_{max} = maximum velocity at each section
$\overline{u_i u_j}$ = Reynolds stress tensor
$\overline{u_i \theta}$ = turbulent heat fluxes
Yap = original, algebraic form of the Yap term as proposed by Yap (1987)
w = rib width
x_i = Cartesian coordinates (x, y)

Greek symbols

δ_{ij} = Kronecker delta
$\tilde{\varepsilon}$ = isotropic dissipation rate
Θ = temperature
Θ_b = cross-section-averaged fluid temperature
Θ_w = wall temperature
κ = thermal conductivity
μ = fluid dynamic viscosity
ν = fluid kinematic viscosity
ρ = fluid density

Introduction

Rib roughened surfaces are a very efficient and widespread means of cooling internally high pressure turbine components. These components are exposed to very high operating temperatures, largely above their melting point. Rib roughened channels enhance the heat transfer but they create complex recirculating flows. It is consequently important that turbulence models employed in the computation of such flows are able to predict accurately the complex flow and heat transfer characteristics. Most of the numerical studies cited in the literature employed high-Reynolds- number turbulence models with wall-functions. Examples of such works include Archarya *et al.* (1993), Lee *et al.* (1988) and Liou *et al.* (1993). However, it is well-known that such approaches are unsuitable for the predictions of separated flows with heat transfer occurring in internal cooling passages of turbine blades due to the presence of curvature and rotation. Recently, Iacovides and Raisee (1999, 2001) examined the capabilities of low-Re number k-ε and second moment closures in predicting convective heat transfer in various two- and three-dimensional and axi-symmetric rib roughened passages. The results of these studies showed that the most reliable predictions are produced through the use of low-Reynolds-number second-moment closures. These efforts also showed that it was necessary to include in the transport equation for the dissipation rate of turbulence energy, a correction term for the near-wall turbulent length-scales. While the correction term initially introduced by Yap (1987) is generally found to be effective, the explicit appearance of the wall distance is felt to be a disadvantage when it comes to flow computations over complex geometries. In an effort to overcome this problem, Iacovides and Raisee (1999) proposed

a differential form of the Yap term, which is independent of the wall distance.

While the case for the use of second moment closures for heat transfer computations in flows involving corner-induced separation is strong, a more economical way in which the effects of turbulence anisotropy can be considered is through the use of non-linear two equation models. In this approach, only two transport equations for turbulence parameters are involved, and the constitutive stress-strain relationship includes additional non-linear (in terms of the strain rate or vorticity) terms. Another feature of these non-linear models is that the parameter C_μ, used in the determination of the turbulent viscosity, is no longer given the constant value appropriate for flows in local equilibrium, but often becomes a function of the strain rate.

Craft *et al.* (1996) developed the non-linear eddy-viscosity model (NLEVM1), including low-Reynolds-number effects. Moreover, they demonstrated that, in order to exhibit the correct sensitivity to streamline curvature, such a non-linear model must retain cubic terms in the stress-strain relationship. This model was then used to predict a range of applications including flow in curved channels, impinging jet flow etc. In each case it resulted in significant predictive improvements in comparison to that produced by a linear low-Reynolds-number k-ε model (EVM).

Parallel applications of this model in the computation of heat and fluid flow through ribbed passages (Raisee, 1999) showed that severe problems of numerical stability were encountered. Raisee traced these stability problems to the form of the dependence of C_μ on the strain rate, which, in flows over sharp corners, led to very abrupt changes in turbulent viscosity. Raisee overcame these stability problems by smoothing the variation of C_μ, a practice that can contaminate the numerical solution. The resulting comparisons indicated that in flows through ribbed passages, the NLEVM1 returned levels of local wall heat transfer are not only higher than those measured, but also higher than those produced by the EVM. A parallel investigation by Cooper (1997), looking at flow through an abrupt pipe expansion, identified that the excessive levels of heat transfer produced by the NLEVM1 were, at least in part, due to the fact that in regions of low near-wall strain rates, which would inevitably be present in recirculation flows, C_μ exceeded its equilibrium value. By limiting the maximum value of C_μ to that of flows in local equilibrium, Cooper was able to improve the thermal predictions of the NLEVM1 in the abrupt pipe expansion, though those of the EVM were still in closer agreement with the experimental data.

More recently, Craft *et al.* (1999) undertook a numerical study to further improve the thermal predictions of cubic low-Reynolds-number two equation model. To pursue this aim, they concentrated on two types of test cases namely: a round jet flow impinging on a heated flat plate and flow over an abrupt pipe

expansion. Craft *et al.* (1999) introduced two modifications to the NLEVM1 proposed by Craft *et al.* (1996). These modifications are:

(1) The introduction of an alternative formulation for the turbulent viscosity parameter C_μ with strain rate, and

(2) The replacement of the Yap algebraic length-scale correction term with a modified form of Iacovides and Raisee (1999) differential length-scale correction term.

The proposed model not only improved the heat transfer predictions in both pipe-expansion and impinging jet, but also removed the need for an explicit wall distance to be prescribed in the model.

The objective of present study is to examine the capabilities of the modified cubic low-Reynolds-number two equation model, proposed by Craft *et al.* (1999) (NLEVM2), in predicting convective heat transfer in two-dimensional and axi-symmetric rib roughened passages.

Cases examined

As shown in Figures 1 and 2, in these investigations fluid flow and heat transfer through two types of passages have been examined: a plane channel with ribs only along one wall and a ribbed pipe.

Five cases have been computed in total, with the details presented in Table I. As shown in Figures 1 and 2, h denotes the rib height, p the rib spacing, D the pipe diameter and H the channel height.

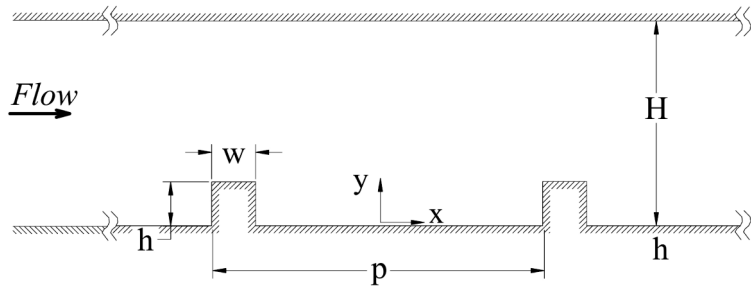

Figure 1.
Longitudinal cross-section of the ribbed plane channel

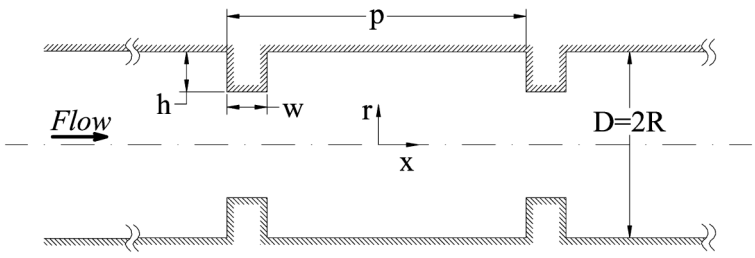

Figure 2.
Longitudinal cross-section of the ribbed pipe

The flow Reynolds number is defined based on the mean streamwise velocity and the channel height (or diameter of the pipe). Here, the local Nusselt number is defined as:

$$\mathrm{Nu} = \frac{q_w D(\text{or } H)}{\kappa(\Theta_w - \Theta_b)}, \tag{1}$$

where D (or H) is the diameter of the pipe (or the channel height), κ the thermal conductivity of the fluid, q_w the wall heat flux, Θ_w the wall temperature and Θ_b the cross-section averaged fluid temperature which is obtained from:

$$\Theta_b = \frac{\int_A \Theta U \, dA}{\int_A U \, dA}. \tag{2}$$

For all test cases, except the ribbed channel at $\mathrm{Re} = 40{,}000$, a constant heat flux boundary condition was assumed for the duct walls and rib surfaces. In accordance with the experimental measurements of Iacovides *et al.* (1998) for the ribbed channel at $\mathrm{Re} = 40,000$ adiabatic and constant heat flux boundary conditions were applied on the smooth and ribbed walls, respectively. For the ribs, a uniform heat flux was imposed on their base and conduction equation was solved across the rib area protruding into the fluid.

Flow equation

All the flow equations are presented in Cartesian tensor notation.

(1) *Mean flow equations*. For a steady incompressible flow, the conservation laws of mass, momentum and energy may be written as:

Continuity:

$$\frac{\partial U_i}{\partial x_i} = 0, \tag{3}$$

Momentum:

$$\frac{\partial (U_j U_i)}{\partial x_j} = -\frac{1}{\rho}\frac{\partial P}{\partial x_i} + \frac{\partial}{\partial x_j}\left(\nu \frac{\partial U_i}{\partial x_j} - \overline{u_i u_j}\right), \tag{4}$$

Passage geometry	p/h	h/H or h/D	Re	Pr	Exp. data	Comparisons
Ribbed channel	9	0.1	30,000	0.71	Rau *et al.* (1998)	Velocity profile
Ribbed channel	10	0.1	122,400	0.71	Purchase (1991)	Local Nu
Ribbed channel	10	0.1	40,000	5.45	Iacovides *et al.* (1998)	Local Nu
Ribbed pipe	18	0.0625	24,000	0.71	Baughn and Roby (1992)	Local Nu
Ribbed pipe	18	0.0625	63,400	0.71	Baughn and Roby (1992)	Local Nu

Table I. Details of cases computed

Energy:

$$\frac{\partial(U_j\Theta)}{\partial x_j} = \frac{\partial}{\partial x_j}\left(\frac{\nu}{\mathrm{Pr}}\frac{\partial\Theta}{\partial x_j} - \overline{u_j\theta}\right). \tag{5}$$

(2) *Turbulence modeling equations*. The turbulence models employed are the widely used Launder and Sharma (1974) low Reynolds number k-ε model (EVM) and a new version of the non-linear low Reynolds number k-ε (Craft *et al.*, 1999) (NLEVM2). Computations with these models have been carried out with the originally proposed (algebric) Yap correction term (Yap, 1987) and also the new version of differential form (NYap), which is free from any explicit wall distance (Iacovides and Raisee, 1999).

Linear low Reynolds number k-ε model

In this turbulence model, the Reynolds stresses and heat fluxes are obtained from the eddy-viscosity and eddy-diffusivity approximations, respectively:

$$\overline{u_iu_j} = \frac{2}{3}\delta_{ij}k - \nu_\mathrm{t}\left(\frac{\partial U_i}{\partial x_j} + \frac{\partial U_j}{\partial x_i}\right), \tag{6}$$

$$-\overline{u_i\theta} = \frac{\nu_\mathrm{t}}{\sigma_\theta}\frac{\partial\Theta}{\partial x_i}, \tag{7}$$

where the turbulent viscosity, ν_t, is obtained from:

$$\nu_\mathrm{t} = C_\mu f_\mu \frac{k^2}{\tilde{\varepsilon}}. \tag{8}$$

and the value of constants C_μ and σ_θ are given in Table II.

To obtain ν_t, transport equations for the turbulence kinetic energy, k, and its dissipation rate, $\tilde{\varepsilon}$ are solved.

The transport equation for turbulent kinetic energy is written as:

$$\frac{\partial}{\partial x_i}(U_ik) = \frac{\partial}{\partial x_i}\left[\left(\nu + \frac{\nu_\mathrm{t}}{\sigma_k}\right)\frac{\partial k}{\partial x_i}\right] + P_k - \tilde{\varepsilon} - 2\nu\left(\frac{\partial\sqrt{k}}{\partial x_i}\right)^2. \tag{9}$$

The dissipation rate of turbulent kinetic energy is obtained by solving the equation:

Table II.
Empirical constants for the k-ε model

$C_{\varepsilon1}$	$C_{\varepsilon2}$	C_μ	σ_k	σ_ε	σ_θ
1.44	1.92	0.09	1.0	1.3	0.9

$$\frac{\partial}{\partial x_i}(U_i\tilde{\varepsilon}) = \frac{\partial}{\partial x_i}\left[\left(\nu + \frac{\nu_t}{\sigma_\varepsilon}\right)\frac{\partial \tilde{\varepsilon}}{\partial x_i}\right] + C_{\varepsilon 1} f_1 \frac{\tilde{\varepsilon}}{k} P_k - C_{\varepsilon 2} f_2 \frac{\tilde{\varepsilon}^2}{k} + E + S_\varepsilon, \quad (10)$$

where the variable $\tilde{\varepsilon}$ is the homogeneous dissipation rate which can be related to the real dissipation rate through:

$$\tilde{\varepsilon} = \varepsilon - 2\nu\left(\frac{\partial \sqrt{k}}{\partial x_j}\right)^2, \quad (11)$$

and P_k is the generation rate of turbulent kinetic energy obtained from:

$$P_k = -\overline{u_i u_j}\frac{\partial U_i}{\partial x_j}. \quad (12)$$

The damping functions f_μ, f_1 and f_2 are given by:

$$\begin{aligned} f_\mu &= \exp[-3.4/(1 + 0.02\tilde{R}_t)^2], \\ f_1 &= 1, \\ f_2 &= 1 - 0.3\ \exp(-\tilde{R}_t^2), \end{aligned} \quad (13)$$

where $\tilde{R}_t = k^2/\nu\tilde{\varepsilon}$ is the local turbulent Reynolds number.

The model constants are given in Table II.

The term E was first introduced by Jones and Launder (1972) and is expressed as:

$$E = 2\nu\nu_t\left(\frac{\partial^2 U_i}{\partial x_j \partial x_k}\right)^2. \quad (14)$$

The extra source term, S_ε, stands for the Yap correction term which is discussed in the later sections.

Non-linear low Reynolds number k-ε model

In this turbulence model, turbulent stresses are obtained via the constitutive relation:

$$\begin{aligned} \overline{u_i u_j} = {} & \frac{2}{3}k\delta_{ij} - \nu_t S_{ij} + C_1\frac{\nu_t k}{\tilde{\varepsilon}}(S_{ik}S_{kj} - 1/3 S_{kl}S_{kl}\delta_{ij}) \\ & + C_2\frac{\nu_t k}{\tilde{\varepsilon}}(\Omega_{ik}S_{kj} + \Omega_{jk}S_{ki}) + C_3\frac{\nu_t k}{\tilde{\varepsilon}}(\Omega_{ik}\Omega_{jk} - 1/3\Omega_{lk}\Omega_{lk}\delta_{ij}) \\ & + C_4\frac{\nu_t k^2}{\tilde{\varepsilon}^2}(S_{ki}\Omega_{lj} + S_{kj}\Omega_{li})S_{kl} \quad + C_5\frac{\nu_t k^2}{\tilde{\varepsilon}^2}(\Omega_{il}\Omega_{lm}S_{mj} + S_{il}\Omega_{lm}\Omega_{mj} \\ & - \frac{2}{3}S_{lm}\Omega_{mn}\Omega_{nl}\delta_{ij}) \quad + C_6\frac{\nu_t k^2}{\tilde{\varepsilon}^2}S_{ij}S_{kl}S_{kl} + C_7\frac{\nu_t k^2}{\tilde{\varepsilon}^2}S_{ij}\Omega_{kl}\Omega_{kl}, \end{aligned} \quad (15)$$

where S_{ij} and Ω_{ij} are strain and vorticity rate tensors:

$$S_{ij} = \left(\frac{\partial U_i}{\partial x_j} + \frac{\partial U_j}{\partial x_i}\right), \quad \Omega_{ij} = \left(\frac{\partial U_i}{\partial x_j} - \frac{\partial U_j}{\partial x_i}\right). \tag{16}$$

The turbulent heat fluxes, $\overline{u_i\theta}$, are modelled using the simple eddy-diffusivity approximation (equation (7)).

The model coefficients, C_1-C_7, have been calibrated by Craft *et al.* (1993), by reference to several flows, including homogeneous shear flows, swirling flows and curved channel flows. The values of these coefficients are given in Table III.

The k and $\tilde{\varepsilon}$ transport equations and eddy-viscosity formulation are similar to those of EVM; however, the following modifications are proposed by Craft *et al.* (1996, 1999).

(1) *Modeling of* C_μ

In the original NLEVM1 C_μ is a function of the strain and vorticity invariants $\tilde{S}$ and $\tilde{\Omega}$.

$$C_\mu = \frac{0.3}{1 + 0.35\eta^{1.5}}\{1 - \exp[-0.36\ \exp(0.75\eta)]\}, \tag{17}$$

with

$$\tilde{S} = \frac{k}{\tilde{\varepsilon}}\sqrt{0.5S_{ij}S_{ij}}, \quad \tilde{\Omega} = \frac{k}{\tilde{\varepsilon}}\sqrt{0.5\Omega_{ij}\Omega_{ij}}, \tag{18}$$

and $\eta = \max(\tilde{S}, \tilde{\Omega})$.

Owing to the strong dependence of equation (17) on the strain rate, the use of the above C_μ expression in the computation of flows over sharp corners results in instability problems. This problem has been recognized by both Cooper (1997) and Raisee (1999) in their computation of similar flows. To overcome these instability problems, the following form of C_μ function was proposed by Craft *et al.* (1999):

$$C_\mu = \min\left[0.09, \frac{12}{1 + 3.5\eta + f_{\mathrm{RS}}}\right], \tag{19}$$

where

Table III.
Values of coefficients in the non-linear k-ε model

C_1	C_2	C_3	C_4	C_5	C_6	C_7
-0.1	0.1	0.26	$-10C_\mu^2$	0	$-5C_\mu^2$	$5C_\mu^2$

$$f_{\mathrm{RS}} = 0.235[\max(0, \eta - 3.333)]^2 \exp(-\tilde{R}_{\mathrm{t}}/400). \tag{20}$$

(2) *Near wall damping*

In the non-linear two equation model, the viscous damping function of ν_t is provided by the function, f_μ:

$$f_\mu = 1 - \exp\left\{-\left(\frac{\tilde{R}_{\mathrm{t}}}{90}\right)^{1/2} - \left(\frac{\tilde{R}_{\mathrm{t}}}{400}\right)^2\right\}. \tag{21}$$

The near-wall source term E is expressed as:

$$E = \begin{cases} 0.0022\dfrac{\tilde{S}\nu_{\mathrm{t}}k^2}{\tilde{\varepsilon}}\left(\dfrac{\partial^2 U_i}{\partial x_k \partial x_l}\right)^2 & \tilde{R}_{\mathrm{t}} \le 250 \\ 0 & \tilde{R}_{\mathrm{t}} > 250 \end{cases} \tag{22}$$

(3) *Length-scale correction terms*

In separated flows, the near-wall length-scale becomes too large, resulting in excessively high levels of near-wall turbulence. To overcome this behavior, Yap (1987) introduced an extra source term into the dissipation rate equation which is based on the wall distance y:

$$S_\varepsilon = \mathrm{Yap} = 0.83\frac{\tilde{\varepsilon}^2}{k}\max[(l/l_{\mathrm{e}} - 1)(l/l_{\mathrm{e}})^2,\ 0], \tag{23}$$

where l is the turbulent length-scale, $k^{3/2}/\tilde{\varepsilon}$, the equilibrium length-scale $l_{\mathrm{e}} = 2.55y$ and y is the distance to the wall.

To eliminate the dependence of the above source term on the wall distance, a differential form of the length-scale correction was proposed by Iacovides and Raisee (1999):

$$S_\varepsilon = \mathrm{NYap} = \max\left[C_\omega F(F+1)^2\frac{\tilde{\varepsilon}^2}{k},\ 0\right] \tag{24}$$

where

$$F = \{[(\partial l/\partial x_j)(\partial l/\partial x_j)]^{1/2} - \mathrm{d}l_{\mathrm{e}}/\mathrm{d}y\}/C_l, \tag{25}$$

represents the difference between the predicted length-scale gradient, with $l = k^{3/2}/\tilde{\varepsilon}$, and the "equilibrium length-scale gradient", $\mathrm{d}l_{\mathrm{e}}/\mathrm{d}y$, defined by:

$$\mathrm{d}l_{\mathrm{e}}/\mathrm{d}y = C_l[1 - \exp(-B_\varepsilon\tilde{R}_{\mathrm{t}})] + B_\varepsilon C_l\tilde{R}_{\mathrm{t}}\ \exp(-B_\varepsilon\tilde{R}_{\mathrm{t}}), \tag{26}$$

where $C_l = 2.55$, $B_\varepsilon = 0.1069$ and $C_\omega = 0.83$.

In order to reduce the amount of correction in the regions of high η, a modified version of the Iacovides and Raisee differential correction term was proposed by Craft *et al.* (1999), where the coefficient C_ω is taken as:

$$C_\omega = \frac{0.83\min(1, \tilde{R}_t/5)}{[0.8 + 0.7(\eta'/3.33)^4 \exp(-\tilde{R}_t/12.5)]}, \quad (27)$$

where the quantity η' is defined in the same way as η but, to enhance stability, the Kolmogorov timescale is used as a lower limit on the timescale $k/\tilde{\varepsilon}$ employed in the expressions for $\tilde{S}$ and $\tilde{\Omega}$, in a manner similar to the proposal of Durbin (1991):

$$\tilde{S} = \max\left[k/\tilde{\varepsilon}, \sqrt{\nu/\varepsilon}\right]\sqrt{\frac{1}{2}S_{ij}S_{ij}}, \quad \tilde{\Omega} = \max\left[k/\tilde{\varepsilon}, \sqrt{\nu/\varepsilon}\right]\sqrt{\frac{1}{2}\Omega_{ij}\Omega_{ij}}. \quad (28)$$

The limited $\tilde{R}_t$ dependent damping is included for numerical stability.

Numerical method

The general form of the governing equations of mean flow, temperature and turbulence fields may be written as:

$$\frac{\partial}{\partial x}\left(\rho r_c^m U\phi\right) + \frac{\partial}{\partial y}\left(\rho r_c^m V\phi\right) = \frac{\partial}{\partial x}\left(\Gamma^\phi r_c^m \frac{\partial \phi}{\partial x}\right) + \frac{\partial}{\partial y}\left(\Gamma^\phi r_c^m \frac{\partial \phi}{\partial y}\right) + r_c^m S^\phi \quad (29)$$

where x and y represent the coordinates in the stream-wise and cross-stream (or radial) directions, respectively, r_c is the radius of curvature, and the index m equals one for the axisymmetric flows and zero for the plane cases. Γ^Φ is an effective diffusion coefficient and S^Φ denotes the source term. In the present study, the above transport equation is solved using finite-volume methodology in a semi-staggered grid system, which is shown in Figure 3. In this arrangement, both velocity components (U, V) are located at the same nodal position which is staggered in relative to the pressure nodes. All the Reynolds stresses and scalars are stored at the pressures nodes. The mean velocity gradient terms that appear in the equations for k, ε and the Reynolds stresses are thus discretised at the scalar nodal locations from the four surrounding velocity nodes. The hybrid differencing of Spalding (1972) is used for the approximation of the convective terms. The pressure field is linked to that of velocity through the well-known SIMPLE, pressure correction algorithm. To avoid stability problems associated with pressure-velocity decoupling, a form of the Rhie and Chow (1983) interpolation scheme, suitable for a semi-staggered mesh, is also employed. The details of the above-mentioned numerical methods are described by Raisee (1999). The fact that a low-Reynolds-number non-linear model of turbulence was used necessitated the introduction of several stabilisation measures.

In the discretization of the mean momentum equations, the turbulent stresses are decomposed into two components: the enhanced linear component

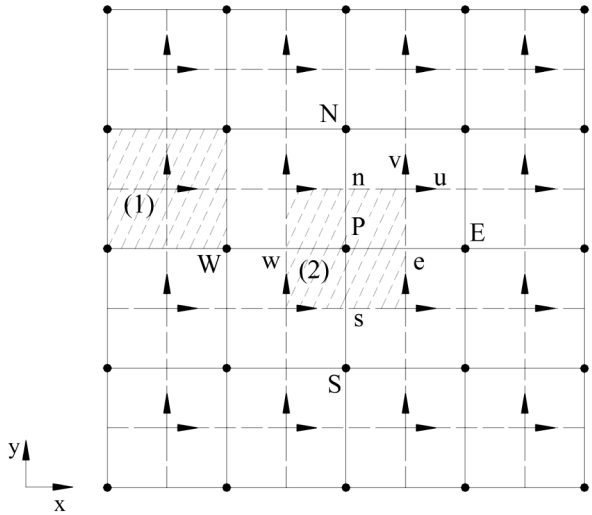

Figure 3.
A partially staggered grid arrangement. (1) Velocity cell, and (2) pressure cell

which, when possible, includes contributions from the last two cubic terms, and the higher order component, $\overline{u_i u_j}$, defined by:

$$\overline{u_i u_j} = \frac{2}{3}k\delta_{ij} - \nu'_t S_{ij} + \overline{u_i u_j},$$

with

$$\nu'_t = \nu_t - \frac{\nu_t k^2}{\tilde{\varepsilon}^2}\min[(C_6 S_{kl}S_{kl} + C_7\Omega_{kl}\Omega_{kl}), 0]. \tag{30}$$

This decomposition was obtained by noting that the linear and the final two cubic terms in equation (15) can be written as:

$$-\left(\nu_t - \frac{\nu_t k^2}{\tilde{\varepsilon}^2}(C_6 S_{kl}S_{kl} + C_7\Omega_{kl}\Omega_{kl})\right)S_{ij}. \tag{32}$$

The enhanced linear component is then directly absorbed into the turbulent diffusion, employing an effective viscosity $(\nu + \nu'_t)$, and only the gradients of the remaining non-linear components appear explicitly in source term S_U. The mean momentum equation is thus written as:

$$\frac{\partial}{\partial x_j}(U_i U_j) = -\frac{1}{\rho}\frac{\partial P}{\partial x_i} + \frac{\partial}{\partial x_j}[(\nu + \nu'_t)S_{ij} - \overline{u_i u_j}]. \tag{33}$$

In the discretization of the k transport equation, the near-wall dissipation term, $2\nu(\partial k^{1/2}/\partial x_j)^2$, is always divided by the existing (previous iteration) value of k at node P and transferred to the left-hand side of the discretized transport equation, making a positive contribution to the diagonal coefficient A_P.

The difference between the generation rate of the turbulent kinetic energy P_k and the dissipation rate $\tilde{\varepsilon}$ is also similarly treated when is negative:

$$A'_P = A_P + [2\nu\left(\partial k^{1/2}/\partial x_j\right)^2_P - \min(P_k - \tilde{\varepsilon}, 0)_P]\frac{\mathrm{Vol}}{k^\circ_P}, \tag{34}$$

$$S_u = \max(P_k - \tilde{\varepsilon}, 0)_P \mathrm{Vol}, \tag{35}$$

where k°_P is the existing value of k at node P, and Vol is the cell volume.

In the discretization of the transport equation for the dissipation rate, the difference between the generation and destruction rate of $\tilde{\varepsilon}$ is also absorbed into the diagonal coefficient A_P when negative:

$$A'_P = A_P - \min(C_{\varepsilon 1}P_k - C_{\varepsilon 2}\tilde{\varepsilon}, 0)_P \frac{\mathrm{Vol}}{k_P}, \tag{36}$$

$$S'_u = S_u + \max(C_{\varepsilon 1}P_k - C_{\varepsilon 2}\tilde{\varepsilon}, 0)_P \frac{\tilde{\varepsilon}^\circ_P}{k_P}\mathrm{Vol}. \tag{37}$$

The cases examined involved passages that are long enough for repeating flow conditions to prevail over each rib interval. Consequently, the numerical flow domain covers only one rib interval, and repeating flow and thermal boundary conditions are applied. The repeating flow boundary conditions are imposed by first applying uniform bulk corrections on velocity and pressure at the exit plane, to satisfy the mass continuity, and then setting the entry conditions same as those at the exit plane. For the temperature field, the temperature distribution at the entry plane is set equal to that at the exit plane, but with a bulk adjustment which maintains a constant temperature at a reference point, within the entry plane.

Computations were performed on a fine grid (91×110), with 37 cells on the rib height. The first grid point is located at $y^* \approx 0.1\left(y^* = y\sqrt{k}/\nu\right)$. In Figure 4, Nusselt numbers obtained using the EVM on a coarse grid (51×60), fine grid

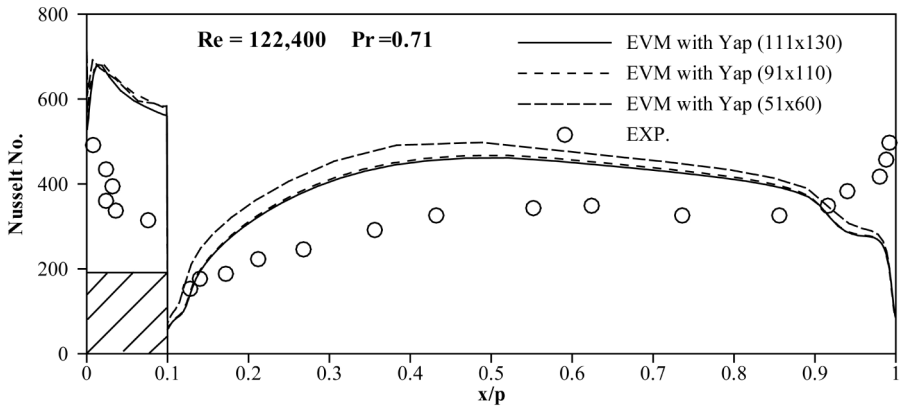

Figure 4.
Predicted distribution of the local Nusselt number through the ribbed plane channel

(91 × 110), and a finer grid (111 × 130) are presented. Though grid refinements from the medium grid to the fine grid caused some differences in the heat transfer predictions, computations on a finer mesh (111 × 130) showed no significant difference in the local Nusselt number distribution. Consequently, results obtained on the 91 × 110 mesh are regarded as grid independence. All the flow and heat transfer computations, presented in the subsequent section, have been obtained on the 91 × 110 mesh. More details can be found in the work of Raisee (1999).

Results and discussion

The predicted velocity vectors and streamlines, using the EVM and NLEVM2 with the NYap term, for flow through the ribbed duct in Re = 30,000 and 122,400, are shown in Figure 5. The vector plot for the ribbed channel indicates that the oncoming flow separates at the front corner of the rib and then reattaches on the wall downstream of the rib. As a result of this process, a large recirculation bubble is created. Downstream of the reattachment point, the entrained flow builds up a new boundary layer. The latter is accelerated by the main stream through the shear forces, impinges on the next rib and forms a smaller recirculation bubble. There is a good agreement between measured and calculated recirculation lengths. The recirculation lengths predicted by the EVM and NLEVM2 are about 4.5 and 4.8 times the rib height, respectively, which are close to the measured value of 4.3 times of the rib height reported by Rau *et al.* (1998). Mean flow predictions for the ribbed channel at Re = 122, 400 indicated that increasing Reynolds number has insignificant effects on the flow features. The predicted velocity vectors and streamlines for the ribbed pipe are similar and are thus not shown here.

In Figure 6, the predicted streamwise velocity profiles for the ribbed channel at Re = 30,000 using the EVM and NLEVM2 with the NYap are compared with the measured data of Rau *et al.* (1998). The mean flow field predictions of both models seem to be similar and there is a good agreement between predictions and experimental data everywhere except over the rib, where the predicted rise in velocity with wall distance is not as steep as that measured.

The performance of the EVM and NLEVM1 in predicting the thermal field through the ribbed pipe and ribbed plane channel at higher Re numbers are shown in Figure 7 (Raisee, 1999). It should be mentioned that the computations were carried out with the original form of the Yap correction term in the dissipation rate equation. For both test cases, over most of the rib interval, the NLEVM1 overestimates the measured Nusselt number levels and also returns the wrong variation, predicting higher Nu levels over the second half of the interval. The EVM, on the other hand, produces the right distribution and also reasonable Nusselt number levels. The predicted location of the maximum wall heat transfer coefficient, using the NLEVM1, is about 25 per cent further downstream compared to that of the EVM.

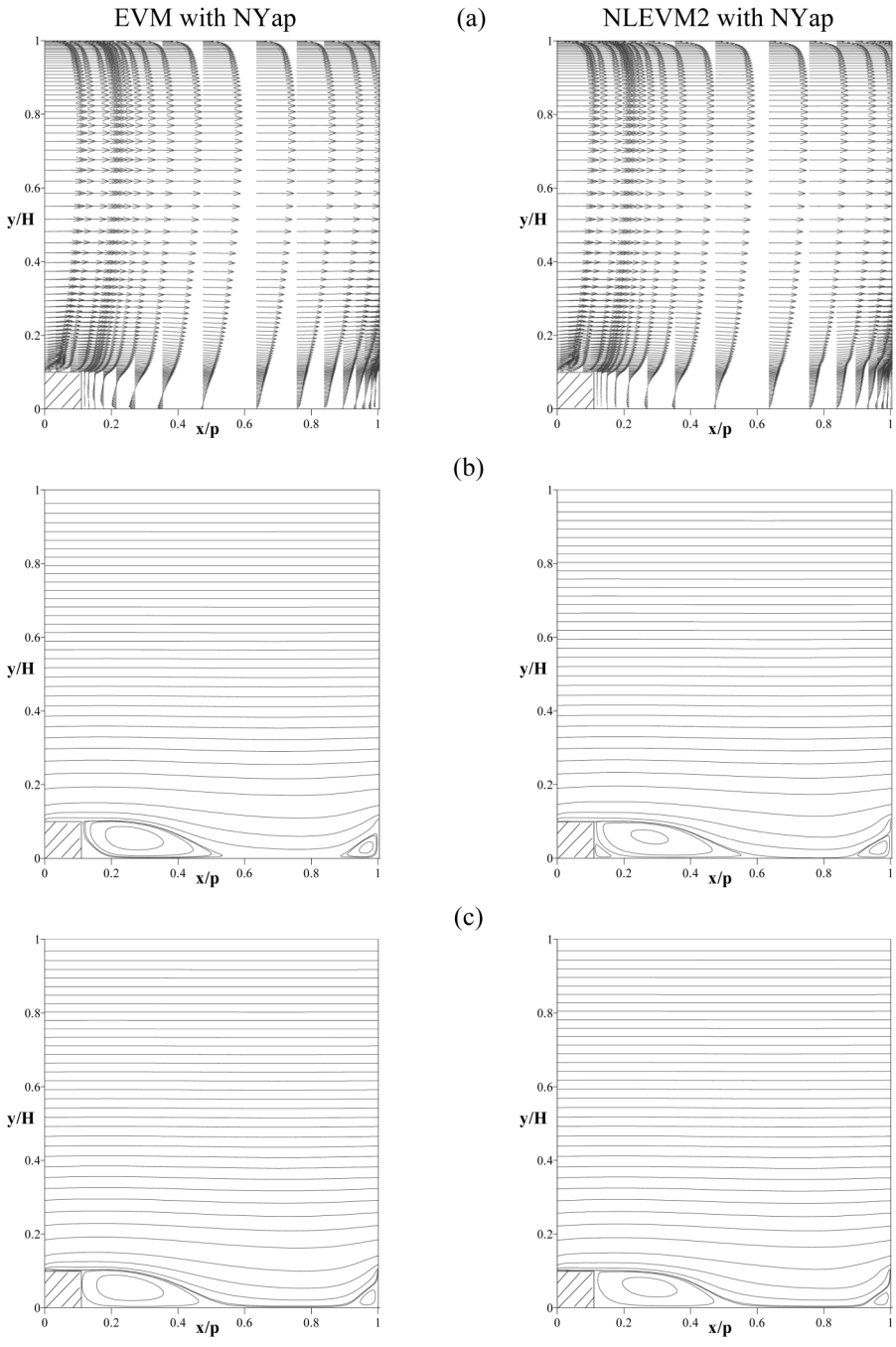

Figure 5.
Predicted velocity vectors and streamlines in a ribbed channel at (a, b) Re = 30,000, and (c) Re = 122,400

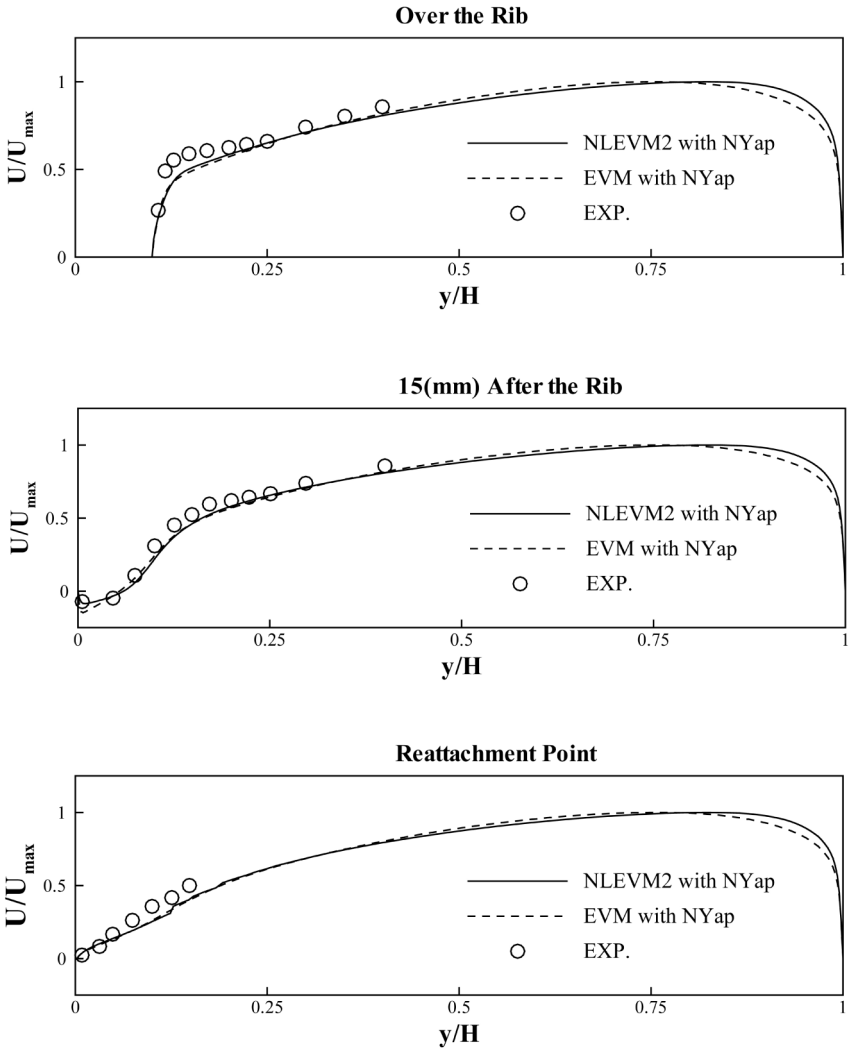

Figure 6.
Velocity profiles for the ribbed channel at Re = 30,000

Figure 8 shows comparisons between measured and predicted Nusselt number distributions, for the NLEVM2. A comparison with the Nu predictions of Figure 7 shows that the NLEVM2 results in considerable predictive improvements in comparison to the NLEVM1. Not only the actual Nusselt number levels are now closer to those measured, but the predicted variation in Nusselt number over the rib interval is also in closer accord with the data. Moreover, this predictive improvement is observed at all Reynolds numbers and both ribbed passage geometries examined. Figure 8 also reveals that the

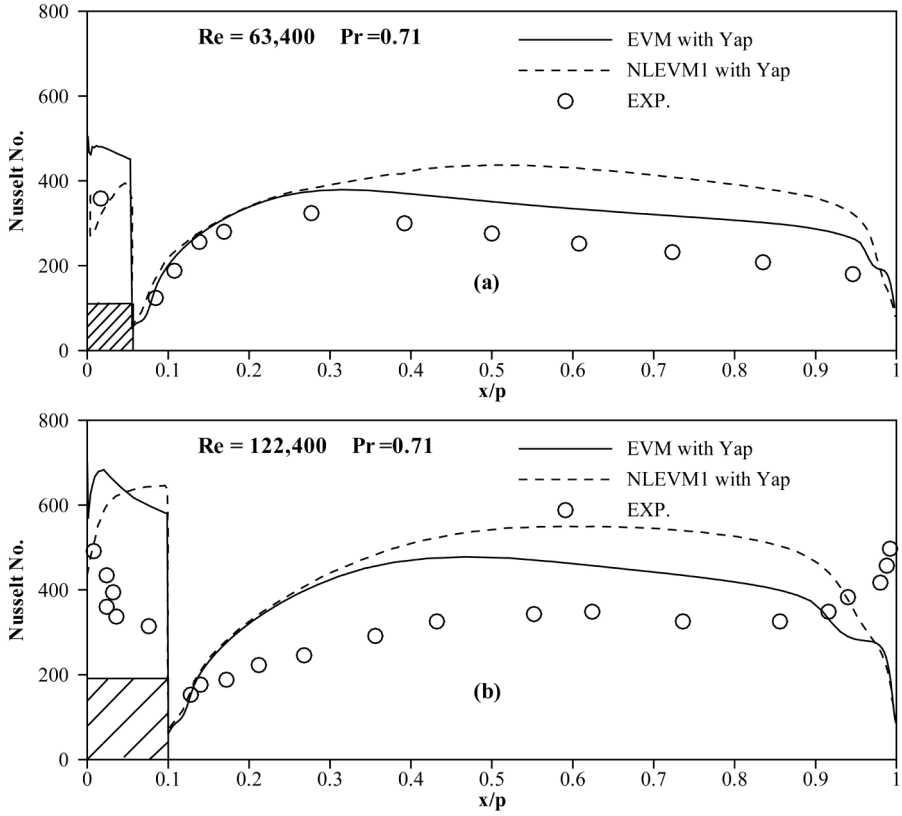

Figure 7.
Predicted distribution of the local Nusselt number through: (a) ribbed pipe, and (b) ribbed plane channel (Raisee, 1999)

thermal predictions of the non-linear k-ε are further improved when the original form of the Yap term is replaced by the differential form (NYap) proposed by Craft *et al.* (1999). These predictive improvements are also observed for all the cases computed.

In Figure 9, the local Nusselt numbers obtained using EVM and NLEVM2 with the NYap are compared with the measured data. The relatively small differences between the two sets of predictions and also the close overall agreement between both sets of predictions and the measurements are in marked contrast to the comparisons of Figure 7. The larger differences between the two sets of predictions appear to be for the ribbed pipe and ribbed channel, at the lowest Reynolds numbers of Re $= 24,000$ and 40,000, respectively. Here, the non-linear model first returns a very gradual rise in Nusselt number in the separation bubble after the rib and further downstream, after reattachment, it predicts Nusselt number levels higher than those of the EVM. These predictive differences between the NLEVM2 and the linear EVM tend to diminish at the higher Reynolds numbers.

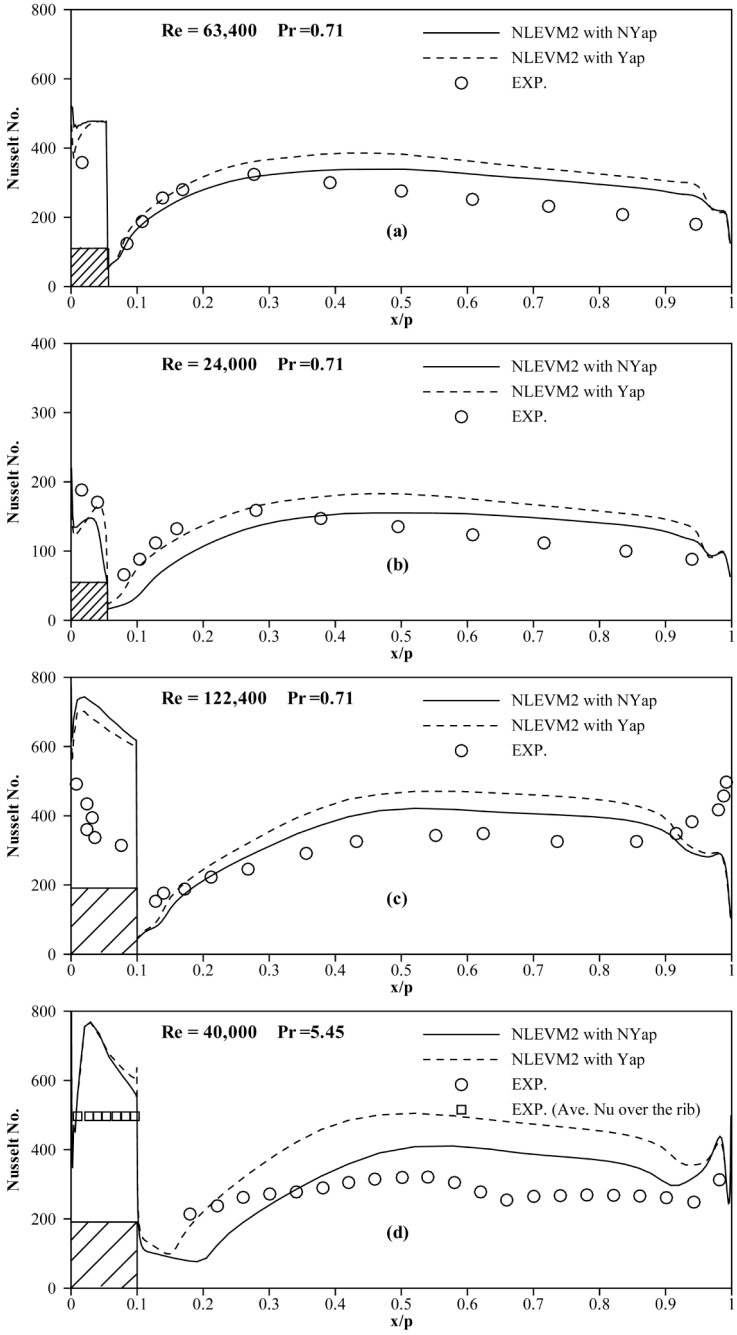

Figure 8.
Predicted distribution of the local Nusselt number through: (a, b) ribbed pipe, and (c, d) ribbed plane channel

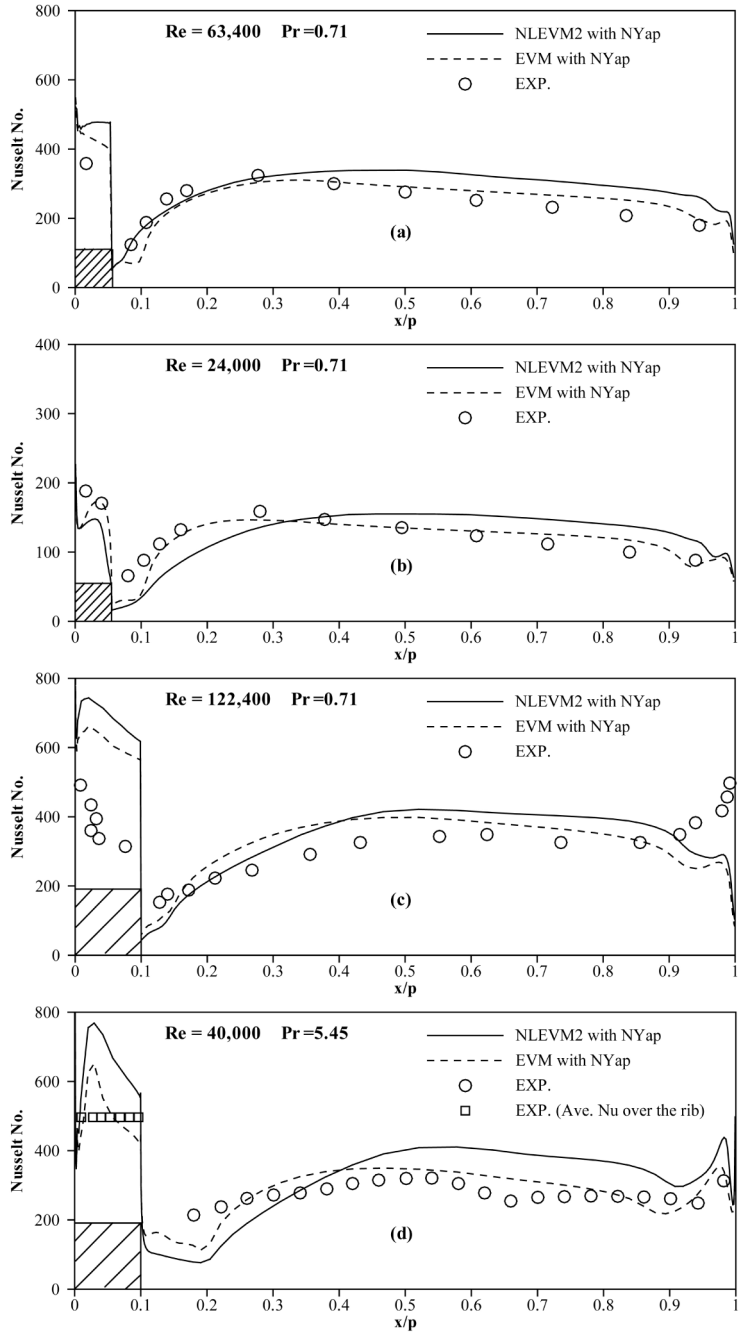

Figure 9.
Predicted distribution of the local Nusselt number through: (a, b) ribbed pipe, and (c, d) ribbed plane channel

There is no doubt that the more recent version of the cubic non-linear k-ε (NLEVM2), considerably improves the thermal predictions of the original version (NLEVM1) in the ribbed passages. Besides producing thermal predictions superior to those of the EVM in pipe expansion and impinging jet flows (Craft *et al.*, 1999), this version of the non-linear k-ε is also shown in this study to produce reliable thermal predictions in ribbed passages.

Conclusions

This study has examined the capabilities of a modified version of Craft *et al.* (1996) cubic two-equation model (NLEVM2) in predicting convective heat transfer through rib-roughened passages. From the computational results presented, the following conclusions can be drawn.

- The mean flow predictions of the modified cubic two equation model are similar to those obtained using the EVM.
- The heat transfer predictions of the recent version of cubic non-linear k-ε model (NLEVM2) are markedly closer to the data than those of the original version (NLEVM1). The heat transfer coefficient distribution returned by the NLEVM2 with the Yap algebraic length-scale correction term is similar to the Nusselt distribution obtained in the experiments, but the heat transfer levels are overestimated.
- The replacement of the Yap correction term with the NYap differential length-scale correction term further improves the heat transfer predictions of the NLEVM2.
- At high Reynolds numbers, the predicted Nusselt number levels returned using NLEVM2 with the NYap closely match the measured values within the recirculation region, but still higher in the developing region.
- The version of the non-linear k-ε that earlier studies have shown to produce improved, relative to the linear k-ε, thermal predictions in abrupt pipe expansions and impinging jet flows, is also shown here to produce reliable thermal predictions in ribbed cooling passages.

References

Archarya, S., Dutta, S., Myrum, T.A. and Baker, R.S. (1993), "Periodically developed flow and heat transfer in a ribbed duct", *International Journal of Heat and Mass Transfer*, Vol. 36, pp. 2069-82.

Baughn, J.W. and Roby, J.L. (1992), "Enhanced turbulent heat transfer in circular ducts with transverse ribs", *ASME 28th National Heat Transfer Conference*, Vol. 202, HTD, San Diego, CA.

Cooper, D. (1997), Computation of momentum and heat transfer in a separated flow using low-Reynolds number linear and non-linear k-ε models, MRes Dissertation, Department of Mechanical Engineering, UMIST.

Craft, T.J., Iacovides, H. and Yoon, J.H. (1999), "Progress in the use of non-linear two-equation models in the computation of convective heat transfer in impinging and separated flows", *Flow, Turbulence and Combustion*, Vol. 63, pp. 59-80.

Craft, T.J., Launder, B.E. and Suga, K. (1993), "Models through the use of deformation invariants and non-linear elements", *Proceedings of IAHR, 5th International Symposium on Refined Flow Modeling and Turbulence Measurements*, Paris, pp. 125-32.

Craft, T.J., Launder, B.E. and Suga, K. (1996), "Development and application of a cubic eddy viscosity model of turbulence", *International Journal of Heat and Fluid Flow*, Vol. 17, pp. 108-15.

Durbin, P.A. (1991), "Near-wall turbulence closure modeling without damping function", *Theoretical Computational Fluid Dynamics*, Vol. 3, pp. 1-13.

Iacovides, H. and Raisee, M. (1999), "Recent progress in the computation of flow and heat transfer in internal cooling passages of turbine blade", *International Journal of Heat and Fluid Flow*, Vol. 20, pp. 320-8.

Iacovides, H. and Raisee, M. (2001), "Computation of flow and heat transfer in two-dimensional rib-roughened passages, using low-Reynolds-number turbulence models", *International Journal of Numerical Methods for Heat and Fluid Flow*, Vol. 11, pp. 138-55.

Iacovides, H., Jackson, D.C., Kelemenis, G., Launder, B.E. and Yuan, Y.M. (1998), "Recent progress in the experimental investigation of flow and local wall heat transfer in internal cooling passages of gas-turbine blades", *Proceedings of 2nd International Conference on Turbulent Heat Transfer*, Manchester, UK, Vol. 2, pp. 7.14-7.28.

Jones, W.P. and Launder, B.E. (1972), "The prediction of laminarization with a two equation model of turbulence", *International Journal of Heat and Mass Transfer*, Vol. 15, pp. 301-14.

Launder, B.E. and Sharma, B.I. (1974), "Application of the energy dissipation model of turbulence to the calculation of flow near a spinning disc", *Letters in Heat Mass Transfer*, Vol. 1, pp. 131-8.

Lee, B.K., Cho, N.H. and Chio, Y.D. (1988), "Analysis of periodically fully-developed turbulent flow and heat transfer by k-ε equation model in artificially roughened annulus", *International Journal of Heat and Mass Transfer*, Vol. 31, pp. 1797-806.

Liou, T.M., Hwang, J.J. and Chen, S.H. (1993), "Simulation and measurement of enhanced turbulent heat transfer in a channel with periodic ribs on one principal wall", *International Journal of Heat and Mass Transfer*, Vol. 36, pp. 507-17.

Purchase, G. (1991), Private communication.

Raisee, M. (1999), "Computation of flow and heat transfer through two- and three-dimensional rib-roughened passages", PhD thesis, Department of Mechanical Engineering, UMIST.

Rau, G., Cakan, M., Moeller, D. and Arts, T. (1998), "The effect of periodic ribs on the local aerodynamic and heat transfer performance of a straight cooling channel", *ASME Journal of Turbomachinery*, Vol. 120, pp. 368-75.

Rhie, C.M. and Chow, W.L. (1983), "Numerical study of the turbulent flow past an airfoil with trailing edge separation", *AIAA Journal*, Vol. 21, pp. 1525-32.

Spalding, D.B. (1972), "A novel finite-difference formulation for differential expressions involving both first and second derivatives", *International Journal of Numerical Methods for Engineering*, Vol. 4, pp. 551-9.

Yap, C.R. (1987), "Turbulent heat and momentum transfer in recirculating and impinging flows", PhD thesis, Faculty of Technology, University of Manchester.